

**UCC Library and UCC researchers have made this item openly available.
Please [let us know](#) how this has helped you. Thanks!**

Title	Brilliant angle-independent structural colours preserved in weevil scales from the Swiss Pleistocene
Author(s)	McDonald, Luke T.; Narayanan, Suresh; Sandy, Alec; Saranathan, Vinodkumar; McNamara, Maria E.
Publication date	2020-04-15
Original citation	McDonald, L. T., Narayanan, S., Sandy, A., Saranathan, V. and McNamara, M. E. (2020) 'Brilliant angle-independent structural colours preserved in weevil scales from the Swiss Pleistocene', Biology Letters, 16(4), 20200063 (6 pp). doi: 10.1098/rsbl.2020.0063
Type of publication	Article (peer-reviewed)
Link to publisher's version	https://royalsocietypublishing.org/doi/10.1098/rsbl.2020.0063 http://dx.doi.org/10.1098/rsbl.2020.0063 Access to the full text of the published version may require a subscription.
Rights	© 2020 The Authors. Published by the Royal Society under the terms of the Creative Commons Attribution License http://creativecommons.org/licenses/by/4.0/ , which permits unrestricted use, provided the original author and source are credited. http://creativecommons.org/licenses/by/4.0/
Item downloaded from	http://hdl.handle.net/10468/11859

Downloaded on 2021-11-27T15:11:23Z

Research



Cite this article: McDonald LT, Narayanan S, Sandy A, Saranathan V, McNamara ME. 2020 Brilliant angle-independent structural colours preserved in weevil scales from the Swiss Pleistocene. *Biol. Lett.* **16**: 20200063. <http://dx.doi.org/10.1098/rsbl.2020.0063>

Received: 4 February 2020

Accepted: 13 March 2020

Subject Areas:

evolution, palaeontology, biomaterials, biophysics

Keywords:

photonic nanostructures, structural colours, fossil colours, Pleistocene, weevils

Authors for correspondence:

Luke T. McDonald

e-mail: luke.mcdonald@ucc.ie

Vinodkumar Saranathan

e-mail: vinodkumar.saranathan@aya.yale.edu

Electronic supplementary material is available online at <https://doi.org/10.6084/m9.figshare.c.4929354>.

Brilliant angle-independent structural colours preserved in weevil scales from the Swiss Pleistocene

Luke T. McDonald^{1,2}, Suresh Narayanan³, Alec Sandy³,
Vinodkumar Saranathan^{4,5,6,7} and Maria E. McNamara^{1,2}

¹School of Biological, Earth and Environmental Sciences, University College Cork, Cork T23 TK30, Ireland

²Environmental Research Institute, University College Cork, Cork T23 XE10, Ireland

³Advanced Photon Source, Argonne National Laboratory, Argonne, IL 60439, USA

⁴Division of Science, Yale-NUS College, 138609, Singapore

⁵Department of Biological Sciences, National University of Singapore 117543, Singapore

⁶NUS Nanoscience and Nanotechnology Initiative (NUSNNI-NanoCore), National University of Singapore, 117581, Singapore

⁷Lee Kong Chian Natural History Museum, National University of Singapore, 117377, Singapore

LTM, 0000-0003-0896-1415; MEM, 0000-0003-0968-4624

Extant weevils exhibit a remarkable colour palette that ranges from muted monochromatic tones to rainbow-like iridescence, with the most vibrant colours produced by three-dimensional photonic nanostructures housed within cuticular scales. Although the optical properties of these nanostructures are well understood, their evolutionary history is not fully resolved, in part due to a poor knowledge of their fossil record. Here, we report three-dimensional photonic nanostructures preserved in brightly coloured scales of two weevils, belonging to the genus *Phyllobius* or *Polydrusus*, from the Pleistocene (16–10 ka) of Switzerland. The scales display vibrant blue, green and yellow hues that resemble those of extant *Phyllobius*/*Polydrusus*. Scanning electron microscopy and small-angle X-ray scattering analyses reveal that the subfossil scales possess a single-diamond photonic crystal nanostructure. In extant *Phyllobius*/*Polydrusus*, the near-angle-independent blue and green hues function primarily in crypsis. The preservation of far-field, angle-independent structural colours in the Swiss subfossil weevils and their likely function in substrate matching confirm the importance of investigating fossil and subfossil photonic nanostructures to understand the evolutionary origins and diversification of colours and associated behaviours (e.g. crypsis) in insects.

1. Introduction

Colour is a critical component of inter- and intraspecific visual communication in extant animals, including signalling strategies such as aposematism, mating displays and crypsis [1–4]. Biological photonic nanostructures—integumentary structures that scatter incident light—are a key evolutionary innovation [4–12]; they produce the most vibrant, highly saturated colours known in biological systems and can manipulate the directionality [9,13] and polarization properties [14,15] of scattered light. Such nanostructures are distributed broadly in extant insects and vary in their complexity, ranging from relatively simple multilayer reflectors to more complex three-dimensional architectures that include amorphous networks and highly ordered crystals [10,16–23]. In insects, three-dimensional photonic nanostructures occur exclusively in scale-bearing taxa [10,16–23],

principally Lepidoptera [16,24,25], weevils [26,27], longhorn beetles [28,29] and, occasionally, scarabs [30].

Despite extensive research into the development, function and optical properties of three-dimensional photonic nanostructures in extant insects, and notwithstanding insights from modern phylogenetic analyses [31], the evolution of such structures is poorly resolved [22,25,32,33]. Fossil insects have the potential to inform on this issue but reports of fossil photonic nanostructures are rare. Structurally coloured fossil insects (beetles and moths) are known from Miocene and Eocene deposits, but preserve only multilayer reflectors [34,35]. Fossil scales possessing periodic nanostructures are preserved in Jurassic lepidopterans [36]; these scales feature a fused lumen and their predicted colour originates from thin-film interference [36,37]. Fossilized three-dimensional photonic nanostructures are known only from a single weevil (*Hypera diversipunctata*) from the Pleistocene of Canada that possesses a single-diamond (*Fd-3m*) photonic crystal (PC) structure within its scales [38]. Here, we report the preservation of bright blue and green scales on subfossil specimens of either *Phyllobius* or *Polydrusus* (Curculionidae: Entiminae) from Lobsigensee (late Pleistocene, Switzerland). Using scanning electron microscopy (SEM) and small-angle X-ray scattering (SAXS), we show that the bright colours of these scales are produced by a single-diamond three-dimensional PC structure and have optical properties consistent with substrate matching. The fossil nanostructures, therefore, represent intermediate stages in models for the evolution of three-dimensional photonic nanostructures and confirm the importance of the Pleistocene fossil insect record as a key source of data on the evolution of three-dimensional photonic nanostructures.

2. Material and methods

Specimens L150D-L and L150D-N were recovered from site L150D (a littoral pit) at the locality of Lobsigensee [39], a small lake on the western Swiss plateau (47°01'55" N and 7°17'57" E [40]). Prior to this study, the specimens were extracted from the sediment via sieving and kerosene flotation [39]. The specimens were recovered from the upper 0.825 m of site L150D, corresponding to an age of ca 10 000–13 000 BP [39]. A precise taxonomic determination was not possible, as the specimens comprise only elytra. However, the specimens were identified as belonging to either the genus *Phyllobius* or *Polydrusus* (S. Elias 2019, personal communication), which are closely related [41].

Optical micrographs of the specimens were taken using a Leica S8APO stereomicroscope fitted with a Leica DFC260 digital camera. For SEM, small (1 × 1 mm²) cuticle samples were mounted on an aluminium stub with carbon tape and sputter coated with Au/Pd. Samples were analysed using a FEI Inspect F50FE-SEM at 5 kV.

For SAXS, individual scales were detached manually from the cuticle and positioned in a custom-made aluminium sample holder between two pieces of 0.03 mm thick Kapton tape. Pinhole SAXS (15 µm horizontal × 15 µm vertical) data in transmission geometry were collected at beamline 8-ID-I at the advanced photon source (APS), Argonne National Laboratory as described elsewhere [22,25]. For additional methods, see the electronic supplementary material.

3. Results

Each subfossil specimen comprises a partial elytron of *Phyllobius*/*Polydrusus* exhibiting sparse bright blue to yellow-green scales

that each show 8–10 parallel ridges oriented along the scale axis (figure 1a,b,e,f). Similar colours and axial ridges are evident in the scales of extant *Phyllobius* (see electronic supplementary material, figure S1).

SEM images (figure 1c,d,g,h) reveal that the scales of both subfossil specimens have an elongate spatulate shape (L150D-L: 30.81 ± 1.44 µm × 16.38 ± 1.83 µm; L150D-N: 44.62 ± 3.49 µm × 17.97 ± 1.53 µm) with rounded apical margins. Some scale margins, notably for specimen L150D-L, show the evidence of physical damage, while many scale pedicles are severed (see electronic supplementary material, figure S2). The paucity of preserved scales (relative to extant *Phyllobius*) thus likely reflects fracturing and loss of scales.

Both subfossil specimens preserve an ordered nanostructure within the scale lumen (figure 1d,g,h; see electronic supplementary material, figure S2). This nanostructure was characterized for specimen L150D-L using SAXS (figure 2). The two-dimensional scattering pattern (figure 2a) confirms the polycrystalline nature of the nanostructure, displaying a concentric series of discrete Bragg scattering peaks from variously oriented crystallite domains. The SAXS scattering profile (figure 2b) features discrete Bragg peaks with scattering wave vector positional ratios (q/q_{pk}): $\sqrt{3}$, $\sqrt{8}$, $\sqrt{11}$ and $\sqrt{19}$ (where $q_{pk} = 0.025 \text{ nm}^{-1}$ with a width (FWHM) of 0.0041 nm^{-1} ; $N = 1$). These peaks correspond to reflections from the (111), (220), (311) and (331) planes, which are consistent with the single-diamond (*Fd-3m*) space group symmetry [42]. Plotting the reciprocal lattice spacing (S) against the moduli of the assigned Miller indices (figure 2c) confirms the cubic aspect of the nanostructure and highlights the absence of scattering peaks at wave vector positional ratios $\sqrt{4}$ and $\sqrt{20}$ that distinguish the subfossil nanostructure from one with a face-centred cubic (*Fm-3m*) space group symmetry. In addition, it estimates the lattice constant for specimen L150D-L to be 435 nm. This result is consistent with SAXS structural measurements from extant *Phyllobius* and *Polydrusus* (433.41 nm and 440.02 nm, respectively; see electronic supplementary material in [22]).

Spectral measurements of the subfossil specimens exhibit reflectance peaks at 549 ± 5 nm (L150D-L) and 515 ± 4 nm (L150D-N), consistent with extant *Phyllobius* (520–580 nm; see electronic supplementary material, figure S3). We performed finite-difference time-domain (FDTD) simulations optimized to match the mean measured reflectance peak for specimen L150D-L, which indicate that its nanostructure has a mean refractive index (n_{avg}) of 1.11, corresponding to a chitin ($n = 1.56$) volume fraction of 0.20 (cf. extant *Phyllobius* sp. and *Polydrusus* sp., electronic supplementary material of [22]). SAXS reflectance predictions and photonic bandgap analyses calculated using these values are consistent with the observed spectrum for specimen L150D-L (see electronic supplementary material, figure S4).

4. Discussion

The low density of cuticular scales on the Lobsigensee specimens is not representative of extant *Phyllobius*/*Polydrusus*; this, plus the abundant fractured scales and/or scale pedicles, strongly indicates that additional scales were originally present but disarticulated from the elytra during decay and/or transport. This process is likely a major control on the fidelity of the fossil record of three-dimensional photonic structures.

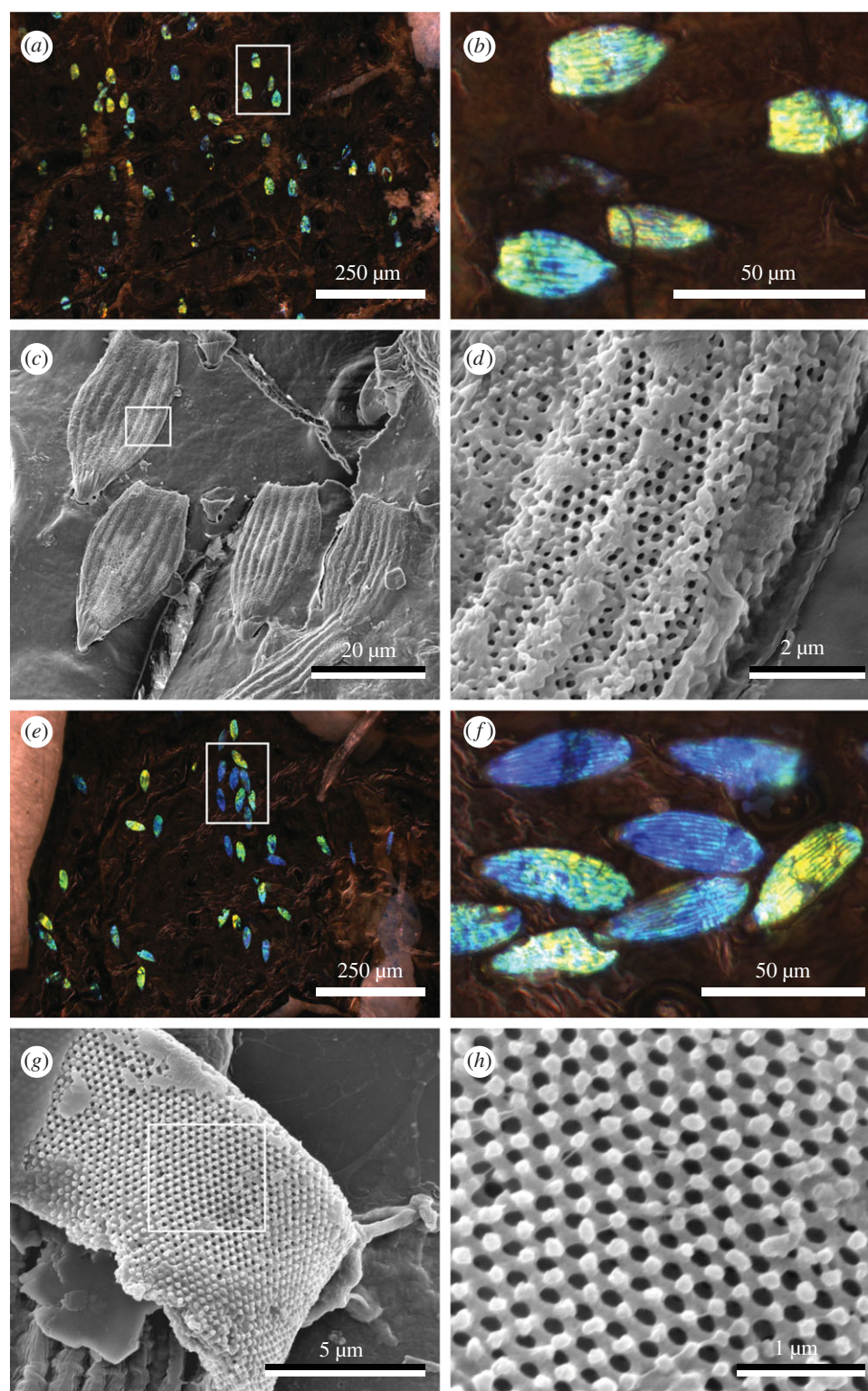


Figure 1. Pleistocene subfossil weevil scales from specimens L150D-L (*a–d*) and L150D-N (*e–h*) imaged using light microscopy (*a,b,e,f*) and SEM (*c,d,g,h*). Light micrographs show the preservation of scales preserving bright blue, green and yellow hues, while electron micrographs reveal three-dimensional photonic nanostructures. (*b,d,f,h*) Regions bounded by white boxes in (*a,c,e,g*; *a,e* rotated 90° clockwise), respectively.

Despite the resistance of such structures to microbial decay and maturation at elevated temperatures and pressures [43], transport-induced scale loss is probably a major taphonomic filter in the early stages of fossilization. Critical information loss, therefore, occurs prior to the delivery of specimens to the site of deposition. Confounding factors may include transport-related biases linked to scale location, geometry and chitin filling fraction. Further, the small size of cuticular scales (particularly when incomplete) renders observation via light microscopy difficult; scales are rarely observed as disarticulated

remains in sediments. An improved understanding of the fossil record and of the evolutionary origins of three-dimensional photonic nanostructures in fossil insects, therefore, requires careful investigation of fossil remains in order to identify any rare, small scales that have survived transport.

The subfossil *Phyllobius*/*Polydrusus* confirm that fossil three-dimensional PCs can produce vivid structural colours with minimal iridescence. Such nanostructures usually produce less angle-dependent colours than one-dimensional thin-film or multilayer reflectors due to the three-dimensional nature

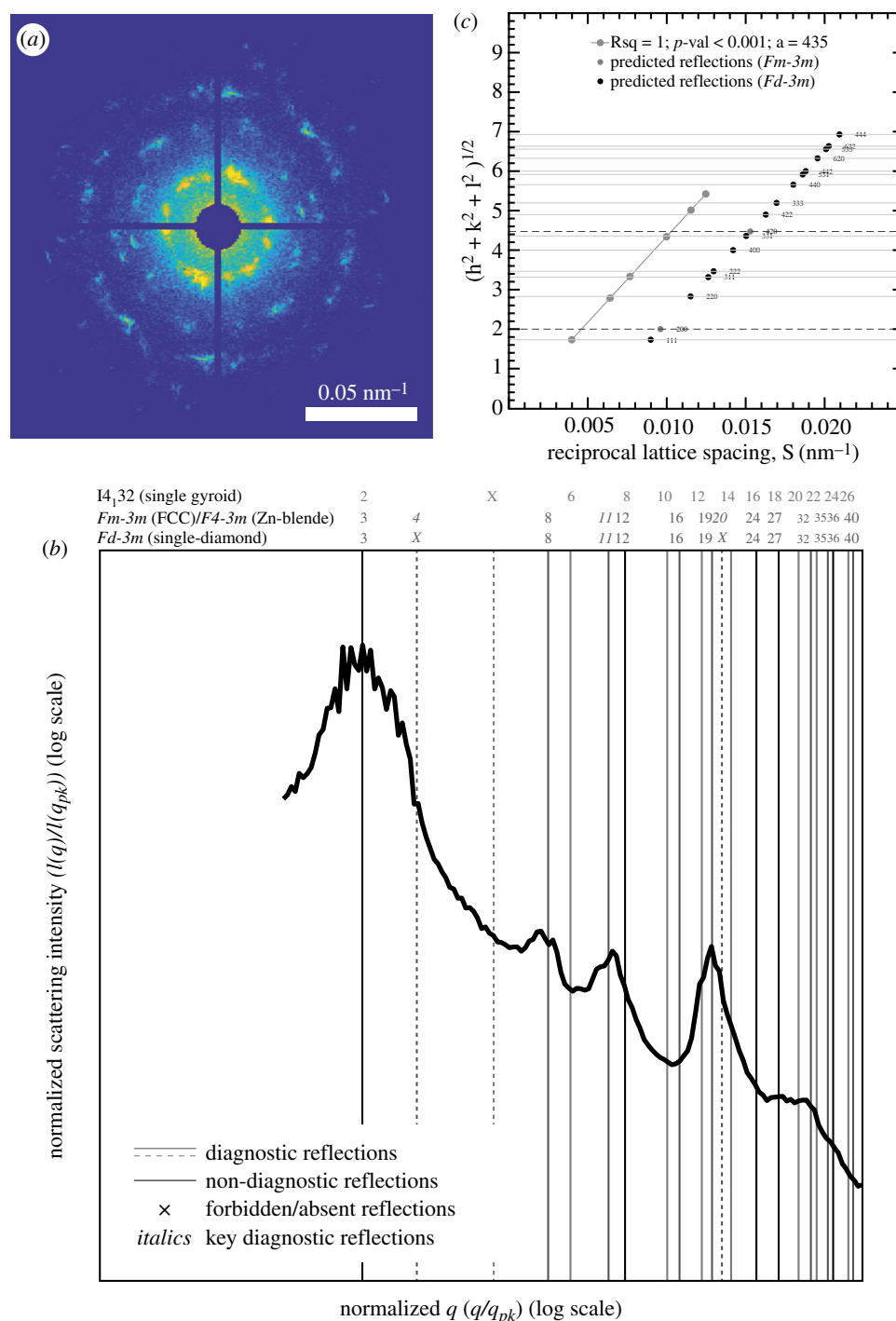


Figure 2. SAXS structural diagnosis of the three-dimensional photonic nanostructure in scales of specimen L150D-L. (a) Two-dimensional SAXS scattering pattern. (b) Normalized, azimuthally averaged SAXS profile integrated from the two-dimensional SAXS pattern in (a). Vertical lines denote expected Bragg peak positional ratios for various alternative cubic crystallographic space groups. Numbers above the lines are the squares of the moduli of the Miller indices (hkl) for the corresponding allowed reflections. The normalized positional ratios of the scattering peaks are indexed to the predictions of specific crystallographic space groups following IUCr conventions [35]. (c) Reciprocal lattice spacing S plotted against the moduli of the Miller indices confirms the cubic aspect of the nanostructure. The absence of experimentally measured Bragg scattering peaks coinciding with characteristic reflections from the $I4_132$ or $Fm\text{-}3m$ symmetries is consistent with the single-diamond diagnosis for the subfossil nanostructure.

of the Brillouin zones of the underlying PCs [44]. In addition, iridescence is modulated by introducing disorder into the structure [27]. Although the Lobsigensee specimens possess an ordered single-diamond structure, the additive mixing of colours from differently oriented crystallites within the scales suppresses iridescence at the macroscopic scale, giving rise to far-field near-angle-independent coloration [26,27,44].

The only other known example of fossil three-dimensional PCs (in the weevil *Hypera* from the Pleistocene of Canada) also comprises a single-diamond PC structure [38]. In contrast

with *Phyllobius*/*Polydrusus*, the preserved *Hypera* scales exhibit an unremarkable reddish-brown macroscopic hue due to the larger lattice constant (*ca* 500 nm (*Hypera*); 435 nm (specimen L150D-L)) of the single-diamond structure, pointillistic mixing of colours from small (*ca* 2 μ m wide) lattice domains and a higher chitin volume fraction (0.44 (*Hypera*); 0.20 (specimen L150D-L)) [38,45].

The diagnosis of a single-diamond PC structure in the subfossil *Phyllobius*/*Polydrusus* specimens is consistent with published SAXS data for extant *Phyllobius* and *Polydrusus*

[22]. Single-diamond PCs are known only in weevils and are considered the dominant photonic structure in entimine weevils [22]. This is supported by recent phylogenetic studies [41,46], with the majority of weevils identified as possessing single-diamond PCs in [22] positioned in the Palaearctic-Oriental (including Phyllobiini) and Neotropical entimine clades. The scales of specimens lacking single-diamond structures instead contain amorphous structures or single gyroid PCs. The broader phylogenetic distribution of three-dimensional PCs in weevils points to a single origin at the base of a clade that groups Entiminae with the subfamily Cyclominae and the tribes Hyperini and Vitiini [33].

Entiminae are the most speciose weevil subfamily. Adults eat young shoots and leaves and typically deposit their eggs on plants, surface litter and/or soil. As a result, entimine weevils have evolved various strategies to facilitate crypsis, including substrate matching. Most (60%; $n=60$) entimine weevils studied in [22] that possess single-diamond PCs have scales with green hues (blue-green to yellow-green). Given the near-angle-independent nature of the hues produced, three-dimensional PCs tuned to scatter green light provide efficient cryptic coloration in foliage over a broad range of angles. The fossil insect and pollen assemblages from Lobsigensee collectively indicate a temperate climate [40] and a eutrophic lake environment colonized by reeds, rushes and sedges [40]. It is therefore likely that the far-field angle-independent bright green hues of the *Phyllobius/Polydrusus* specimens performed a similar function to the matte brown of *H. diversipunctata* by facilitating cryptic substrate matching, in this case with vegetation.

Unlike other camouflage mechanisms used by insects (i.e. disruptive coloration and masquerade), crypsis minimizes the signal/noise ratio between body and background [3,47]. Disruptive coloration is often employed in habitats rich in bark, sand and soil, while crypsis and masquerade (as leaves/twigs) are often used in foliaceous environments [3]. In Coleoptera, the evolution of photonic nanostructures has been key to facilitating crypsis in foliaceous habitats as they lack the green-producing pigments, i.e. bilins, used in other insect orders (e.g. Lepidoptera, Mantodea, Orthoptera, Phasmida) [48]. Indeed, the diffuse far-field green reflectance of the *Entimus imperialis* weevil, which also results from a single-diamond PC, corresponds closely to the reflectance of green leaves [49]. Similarly, some lycaenid butterflies have green coloured ventral

scales (containing a single gyroid three-dimensional PC nanostructure) that provide camouflage when perched with wings closed [50,51].

The key features of the *Phyllobius/Polydrusus* photonic nanostructure, i.e. a single-diamond PC tuned to scatter greenish hues, are a synapomorphy or shared-derived trait of a clade of broad-nosed weevils (predominantly Entiminae) as proposed by Seago *et al.* [31]. Such structures are considered evolutionarily derived relative to the amorphous or spongy nanostructures in brentids and higher weevils but primitive to structures that produce non-cryptic colours, such as in Pachyrhynchini and those with a single gyroid architecture [31]. This hypothesis, therefore, predicts that three-dimensional photonic nanostructures in the scales of higher weevil taxa (i.e. Curculionidae) will be dominated by amorphous nanostructures. In particular, the evolutionary origins of three-dimensional photonic nanostructures in weevil scales has been linked to the proliferation of angiosperms and the associated diversification of weevils in the Early Cretaceous [31,52,53]. Fossil weevils from the Early Cretaceous are thus prime targets for future studies on the evolution of three-dimensional PCs and are essential to test hypotheses on the origin and diversification of ancestral photonic nanostructures and their functions.

Data accessibility. Data used for this analysis can be found either in this article, the electronic supplementary material, or openly accessed here: <https://doi.org/10.5281/zenodo.3677700> (SAXS detector image, raw reflectance spectra).

Authors' contributions. L.T.M. and M.E.M. designed the study with input from V.S., L.T.M. and M.E.M. performed microscopy and collected reflectance measurements. V.S., S.N. and A.S. performed SAXS measurements. V.S. analysed SAXS data and performed optical simulations. All authors discussed the data and results. L.T.M. and M.E.M. wrote the manuscript with input from V.S. All authors reviewed and commented on the final version of the manuscript. All authors gave approval of the final version and agree to be held accountable for the content therein.

Competing interests. We declare we have no competing interests.

Funding. This research was supported by the European Research Council (H2020-2014-ERC-StG-637691-ANICOLEVO to M.E.M.), the US Department of Energy, Office of Science, Office of Basic Energy Sciences (contract DE AC02 06CH11357) and Yale-NUS College start-up funds (to V.S.).

Acknowledgements. The authors thank Scott Elias for donating the sub-fossil specimens and for useful discussions, Aidan O'Hanlon for the loan of modern *Phyllobius* and Aeilish O'Hanlon for assistance with preliminary investigations.

References

- Cuthill IC *et al.* 2017 The biology of color. *Science* **357**, eaan0221. (doi:10.1126/science.aan0221)
- Ruxton GD, Sherratt TN, Speed MP. 2004 *Avoiding attack: the evolutionary ecology of crypsis, warning signals, and mimicry*. Oxford, UK: Oxford University Press.
- Stevens M, Merilaita S. 2011 *Animal camouflage: mechanisms and function*. Cambridge, UK: Cambridge University Press.
- Doucet SM, Meadows MG. 2009 Iridescence: a functional perspective. *J. R. Soc. Interface* **6**, S115–S132. (doi:10.1098/rsif.2008.0395.focus)
- Fox DL. 1976 *Animal biochromes and structural colours: physical, chemical, distributional and physiological features of coloured bodies in the animal world*. Berkeley, CA: University of California Press.
- Parker AR. 1995 Discovery of functional iridescence and its coevolution with eyes in the phylogeny of Ostracoda (Crustacea). *Proc. R. Soc. B* **262**, 349–355. (doi:10.1098/rspb.1995.0216)
- Parker AR. 2000 515 million years of structural colour. *J. Opt. A. Pure. Appl. Opt.* **2**, R15–R28. (doi:10.1088/1464-4258/2/6/201)
- Vukusic P, Sambles JR. 2003 Photonic structures in biology. *Nature* **424**, 852–855. (doi:10.1038/nature1941)
- Wickham S, Large MCJ, Poladian L, Jermy LS. 2006 Exaggeration and suppression of iridescence: the evolution of two-dimensional butterfly structural colours. *J. R. Soc. Interface* **3**, 99–108. (doi:10.1098/rsif.2005.0071)
- Seago AE, Brady P, Vigneron J-P, Schultz TD. 2009 Gold bugs and beyond: a review of iridescence and structural colour mechanisms in beetles (Coleoptera). *J. R. Soc. Interface* **6**, S165–S184. (doi:10.1098/rsif.2008.0354.focus)
- Whitney HM, Kolle M, Andrew P, Chittka L, Steiner U, Glover BJ. 2009 Floral iridescence, produced by diffractive optics, acts as a cue for animal pollinators. *Science* **323**, 130–133. (doi:10.1126/science.1166256)
- Mäthger LM, Denton EJ, Marshall NJ, Hanlon RT. 2009 Mechanisms and behavioural functions of

- structural coloration in cephalopods. *J. R. Soc. Interface* **6**, S149–S163. (doi:10.1098/rsif.2008.0366.focus)
13. Vukusic P, Sambles JR, Lawrence CR, Wootton RJ. 2002 Limited-view iridescence in the butterfly *Ancyluris meliboeus*. *Proc. R. Soc. B* **269**, 7–14. (doi:10.1098/rspb.2001.1836)
 14. Vukusic P, Sambles R, Lawrence C, Wakely G. 2001 Sculpted-multilayer optical effects in two species of *Papilio* butterfly. *Appl. Opt.* **40**, 1116–1125. (doi:10.1364/AO.40.001116)
 15. Finlayson ED, McDonald LT, Vukusic P. 2017 Optically ambidextrous circularly polarized reflection from the chiral cuticle of the scarab beetle *Chrysina resplendens*. *J. R. Soc. Interface* **14**, 20170129. (doi:10.1098/rsif.2017.0129)
 16. Ghiradella H. 1984 Structure of iridescent lepidopteran scales: variations on several themes. *Ann. Entomol. Soc. Am.* **77**, 637–645. (doi:10.1093/aesa/77.6.637)
 17. Ghiradella H. 1998 Hairs, bristles, and scales. In *Microscopic anatomy of invertebrates*, vol. 11A, *Insecta* (ed. M Locke), pp. 257–287. New York, NY: Wiley-Liss.
 18. Srinivasarao M. 1999 Nano-optics in the biological world: beetles, butterflies, birds, and moths. *Chem. Rev.* **99**, 1935–1961. (doi:10.1021/cr970080y)
 19. Prum RO, Quinn T, Torres RH. 2006 Anatomically diverse butterfly scales all produce structural colours by coherent scattering. *J. Exp. Biol.* **209**, 748–765. (doi:10.1242/jeb.02051)
 20. Ingram AL, Parker AR. 2008 A review of the diversity and evolution of photonic structures in butterflies, incorporating the work of John Huxley (The Natural History Museum, London from 1961 to 1990). *Phil. Trans. R. Soc. B* **363**, 2465–2480. (doi:10.1098/rstb.2007.2258)
 21. Kinoshita S, Yoshioka S, Miyazaki J. 2008 Physics of structural colors. *Reports Prog. Phys.* **71**, 076401. (doi:10.1088/0034-4885/71/7/076401)
 22. Saranathan V, Seago AE, Sandy A, Narayanan S, Mochrie SGJ, Dufresne ER, Cao H, Osuji CO, Prum RO. 2015 Structural diversity of arthropod biophotonic nanostructures spans amphiphilic phase-space. *Nano Lett.* **15**, 3735–3742. (doi:10.1021/acs.nanolett.5b00201)
 23. Saranathan V. 2018 Topology of minimal surface biophotonic nanostructures in arthropods. In *Springer series in solid-state sciences: the role of topology in materials* (eds S Gupta, A Saxena), pp. 275–290. New York, NY: Springer.
 24. Michielsen K, Stavenga DG. 2008 Gyroid cuticular structures in butterfly wing scales: biological photonic crystals. *J. R. Soc. Interface* **5**, 85–94. (doi:10.1098/rsif.2007.1065)
 25. Saranathan V, Osuji CO, Mochrie SGJ, Noh H, Narayanan S, Sandy A, Dufresne ER, Prum RO. 2010 Structure, function, and self-assembly of single network gyroid ($I_4/32$) photonic crystals in butterfly wing scales. *Proc. Natl Acad. Sci. USA* **107**, 11 676–11 681. (doi:10.1073/pnas.0909616107)
 26. Galusha JW, Richey LR, Gardner JS, Cha JN, Bartl MH. 2008 Discovery of a diamond-based photonic crystal structure in beetle scales. *Phys. Rev. E* **77**, 050904. (doi:10.1103/PhysRevE.77.050904)
 27. Pouya C, Stavenga DG, Vukusic P. 2011 Discovery of ordered and quasi-ordered photonic crystal structures in the scales of the beetle *Eupholus magnificus*. *Opt. Express* **19**, 11 355–11 364. (doi:10.1364/OE.19.011355)
 28. Simonis P, Vigneron JP. 2011 Structural color produced by a three-dimensional photonic polycrystal in the scales of a longhorn beetle: *Pseudomyagrus waterhousei* (Coleoptera: Cerambycidae). *Phys. Rev. E* **83**, 011908. (doi:10.1103/PhysRevE.83.011908)
 29. Colomer J-F, Simonis P, Bay A, Cloetens P, Suhonen H, Rassart M, Vandenbem C, Vigneron JP. 2012 Photonic polycrystal in the greenish-white scales of the African longhorn beetle *Prosopocera lactator* (Cerambycidae). *Phys. Rev. E* **85**, 011907. (doi:10.1103/PhysRevE.85.011907)
 30. Vukusic P, Hallam B, Noyes J. 2007 Brilliant whiteness in ultrathin beetle scales. *Science* **315**, 348. (doi:10.1126/science.1134666)
 31. Seago AE, Oberprieler R, Saranathan VK. 2019 Evolution of insect iridescence: origins of three-dimensional photonic crystals in weevils (Coleoptera: Curculionidae). *Integr. Comp. Biol.* **59**, 1664–1672. (doi:10.1093/icb/icz040)
 32. Wilts BD, Zubiri BA, Klatt MA, Butz B, Fischer MG, Kelly ST, Spiecker E, Steiner U, Schröder-Turk GE. 2017 Butterfly gyroid nanostructures as a time-frozen glimpse of intracellular membrane development. *Sci. Adv.* **3**, e1603119. (doi:10.1126/sciadv.1603119)
 33. Ghiradella HT, Butler MW. 2009 Many variations on a few themes: a broader look at development of iridescent scales (and feathers). *J. R. Soc. Interface* **6**, S243–S251. (doi:10.1098/rsif.2008.0372.focus)
 34. McNamara ME, Briggs DEG, Orr PJ, Wedmann S, Noh H, Cao H. 2011 Fossilized biophotonic nanostructures reveal the original colors of 47-million-year-old moths. *PLoS Biol.* **9**, e1001200. (doi:10.1371/journal.pbio.1001200)
 35. McNamara ME, Briggs DEG, Orr PJ, Noh H, Cao H. 2012 The original colours of fossil beetles. *Proc. R. Soc. B* **279**, 1114–1121. (doi:10.1098/rspb.2011.1677)
 36. Zhang Q *et al.* 2018 Fossil scales illuminate the early evolution of lepidopterans and structural colors. *Sci. Adv.* **4**, e1700988. (doi:10.1126/sciadv.1700988)
 37. Kilchoer C, Steiner U, Wilts BD. 2018 Thin-film structural coloration from simple fused scales in moths. *Interface Focus* **9**, 20180044. (doi:10.1098/rsfs.2018.0044)
 38. McNamara ME, Saranathan V, Locatelli ER, Noh H, Briggs DEG, Orr PJ, Cao H. 2014 Cryptic iridescence in a fossil weevil generated by single diamond photonic crystals. *J. R. Soc. Interface* **11**, 20140736. (doi:10.1098/rsif.2014.0736)
 39. Elias SA, Wilkinson B. 1983 Lateglacial insect fossil assemblages from Lobsigensee (Swiss Plateau). Studies in the late Quaternary of Lobsigensee 3. *Rev. Paleobiol.* **2**, 189–204.
 40. Ammann B, Tobolski K. 1983 Vegetational development during the Late-Würm at Lobsigensee (Swiss Plateau). Studies in the late Quaternary of Lobsigensee I. *Rev. Paleobiol.* **2**, 163–180.
 41. Marvaldi AE, del Río MG, Pereyra VA, Rocamundi N, Lanteri AA. 2018 A combined molecular and morphological approach to explore the higher phylogeny of entimine weevils (Coleoptera: Curculionidae), with special reference to South American taxa. *Diversity* **10**, d10030095. (doi:10.3390/d10030095)
 42. Hahn T. 2006 The 230 space groups. In *IUCr international tables for crystallography* (eds T Hahn, MI Aroyo), pp. 112–117. Berlin, Germany: Springer.
 43. McNamara ME *et al.* 2013 The fossil record of insect color illuminated by maturation experiments. *Geology* **41**, 487–490. (doi:10.1130/G33836.1)
 44. Poladian L, Wickham S, Lee K, Large MCJ. 2009 Iridescence from photonic crystals and its suppression in butterfly scales. *J. R. Soc. Interface* **6**, S233–S242. (doi:10.1098/rsif.2008.0353.focus)
 45. Wilts BD, Saranathan V. 2018 A literal elytral rainbow: tunable structural colors using single diamond biophotonic crystals in *Pachyrhynchus congestus* weevils. *Small* **14**, 1802328. (doi:10.1002/smll.201802328)
 46. Girón JC, Franz NM. 2010 Revision, phylogeny and historical biogeography of the genus *Apodrosus* Marshall, 1922 (Coleoptera: Curculionidae: Entiminae). *Insect Syst. Evol.* **41**, 339–414. (doi:10.1163/187631210X538799)
 47. Cuthill IC, Stevens M, Sheppard J, Haddocks T, Párraga CA, Troschianko TS. 2005 Disruptive coloration and background pattern matching. *Nature* **434**, 72–74. (doi:10.1038/nature03312)
 48. Shamim G, Ranjan SK, Pandey DM, Ramani R. 2014 Biochemistry and biosynthesis of insect pigments. *Eur. J. Entomol.* **111**, 149–164. (doi:10.14411/eje.2014.021)
 49. Wilts BD, Michielsen K, Kuipers J, De Raedt H, Stavenga DG. 2012 Brilliant camouflage: photonic crystals in the diamond weevil, *Entimus imperialis*. *Proc. R. Soc. B* **279**, 2524–2530. (doi:10.1098/rspb.2011.2651)
 50. Kertész K, Bálint Z, Vértess Z, Márk G, Lousse V, Vigneron JP, Rassart M, Bíró LP. 2006 Gleaming and dull surface textures from photonic-crystal-type nanostructures in the butterfly *Cyanophrys remus*. *Phys. Rev. E* **74**, 021922. (doi:10.1103/PhysRevE.74.021922)
 51. Michielsen K, De Raedt H, Stavenga DG. 2010 Reflectivity of the gyroid biophotonic crystals in the ventral wing scales of the green hairstreak butterfly, *Callophrys rubi*. *J. R. Soc. Interface* **7**, 765–771. (doi:10.1098/rsif.2009.0352)
 52. Oberprieler RG, Marvaldi AE, Anderson RS. 2007 Weevils, weevils, weevils everywhere. *Zootaxa* **1668**, 491–520. (doi:10.11646/zootaxa.1668.1.24)
 53. McKenna DD, Sequeira AS, Marvaldi AE, Farrell BD. 2009 Temporal lags and overlap in the diversification of weevils and flowering plants. *Proc. Natl Acad. Sci. USA* **106**, 7083–7088. (doi:10.1073/pnas.0810618106)